

UC San Diego

UC San Diego Electronic Theses and Dissertations

Title

Aerial photogrammetry to estimate size, growth, and body condition of mammal-eating Bigg's killer whales

Permalink

<https://escholarship.org/uc/item/5sr6482f>

Author

Kotik, Chloe

Publication Date

2020

Peer reviewed|Thesis/dissertation

UNIVERSITY OF CALIFORNIA SAN DIEGO

Aerial photogrammetry to estimate size, growth, and body condition of mammal-eating Bigg's
killer whales

A thesis submitted in partial satisfaction of the
requirements for the degree Master of Science

in

Marine Biology

by

Chloe Kotik

Committee in charge:

Simone Baumann-Pickering, Chair
John Hildebrand
Carolyn Kurle
John Durban
Holly Fearnbach

2020

Copyright
Chloe Kotik, 2020
All rights reserved

The Thesis of Chloe Kotik is approved, and it is acceptable in quality and form for publication on microfilm and electronically:

Chair

University of California San Diego

2020

TABLE OF CONTENTS

Signature Page.....	iii
Table of Contents.....	iv
List of Figures.....	v
List of Tables.....	vii
Acknowledgements.....	ix
Abstract of the Thesis.....	xi
Introduction.....	1
Methods.....	4
Results.....	11
Discussion.....	25
References.....	28

LIST OF FIGURES

- Figure 1: Aerial images of Bigg’s killer whales. Left: Adult male T123A with a fresh harbor seal kill. Right: Adult male T123A and his mother, T123, sharing a harbor seal kill.....3
- Figure 2: Locations of 111 flights over Bigg’s killer whales using an unmanned aerial system in the coastal waters off Northern Vancouver Island (NVI), British Columbia, and the Salish Sea (SS) surrounding the San Juan Islands of Washington State.....5
- Figure 3: John Durban piloting the APO-42 Octocopter (Aerial Imaging Solutions) into the hands of Holly Fearnbach for safe retrieval onboard the R/V *Kohala*. Photo taken by John Calambokidis of the Cascadia Research Collective.....5
- Figure 4: Comparison of saddle pigmentation and scarring patterns used to identify adult female T100 in an aerial image (left) compared to left- and right-side boat-based photo-identification images (Towers et al. 2019).....6
- Figure 5: Aerial images of Bigg’s killer whales showing pixel length measurements conducted in ImageJ on BKW T124A2. Left: upper and lower eye patch measurements (EP TOP and EP BOTTOM, in red) and snout to dorsal insertion (SNDF, in yellow). Right: dorsal insertion to fluke notch (DFFL, in green).....8
- Figure 6: Total length (TL, in meters) estimates of 41 confirmed female (red) and 26 confirmed male (blue) Bigg’s killer whales plotted against known age of individual. The fitted Richard’s growth curves (Equation 1) are plotted for each sex (females in red, males in blue), the parameters of which are described in Table 6, as well as 95% confidence intervals for the model fit.....17
- Figure 7: Eye patch ratio (EPR, a proxy for body condition) values for 44 confirmed female Bigg’s killer whales ranging in age from 0.3 to 52.6 years. Points represent the average values of each individual in each sampling period. Lines represent repeat measurements of the same individual across sampling periods.....20
- Figure 8: Eye patch ratio (EPR, a proxy for body condition) values of 31 confirmed male Bigg’s killer whales ranging in age from 0.6 to 57.3 years. Points represent the average values of each individual in each sampling period. Lines represent repeat measurements of the same individual across sampling periods.....21

Figure 9: Eye patch ratio (EPR, a proxy for body condition) values of 16 Bigg’s killer whales of unknown sex ranging in age from 0.5 to 13.6 years. Points represent the average values of each individual in each sampling period. Lines represent repeat measurements of the same individual across sampling periods.....22

Figure 10: Eye patch ratios (EPR, a proxy for body condition) of 91 individual Bigg’s killer whales: 44 females (ranging in age from 0.3 to 52.6 years, in red), 31 males (ranging in age from 0.6 to 57.3 years, in blue), and 16 of unknown sex (ranging in age from 0.5 to 13.6 years, in gray). Points represent the average values of each individual in each sampling period. Lines represent repeat measurements of the same individual across sampling periods.....23

LIST OF TABLES

- Table 1: Detailed descriptions of each photogrammetry measurement. Measurements in pixels were conducted in ImageJ and subsequently converted to real length estimates.....8
- Table 2: Detailed metrics regarding the year, month, location, duration, and altitude of UAS flights conducted over Bigg’s killer whales in two main regions: the coastal waters of Northern Vancouver Island (NVI), British Columbia, and the Salish Sea (SS) surrounding the San Juan Islands of Washington. Two flights conducted in May of 2018 did not yield duration, altitude, or location data.....11
- Table 3: Whale ID, year and month of capture, sex, altimeter, age, maximum total length (TL), and number of measures for snout to dorsal fin insertion (SNDF) and dorsal fin insertion to fluke (DFFL) of 41 confirmed female Bigg’s killer whales, all taken from the most recent sampling period for each individual. Maximum TL was derived by combining the maximum SNDF and DFFL values measured within a sampling period.....13
- Table 4: Whale ID, year and month of capture, sex, altimeter, age, maximum total length (TL), and number of measures for snout to dorsal fin insertion (SNDF) and dorsal fin insertion to fluke (DFFL) of 26 confirmed male Bigg’s killer whales, all taken from the most recent sampling period for each individual. Maximum TL was derived by combining the maximum SNDF and DFFL values measured within a sampling period.....14
- Table 5: Whale ID, year and month of capture, sex, altimeter, age, maximum total length (TL), and number of measures for snout to dorsal fin insertion (SNDF) and dorsal fin insertion to fluke (DFFL) for 19 Bigg’s killer whales of unknown sex, all taken from the most recent sampling period for each individual. Maximum TL was derived by combining the maximum SNDF and DFFL values measured within a sampling period.....15
- Table 6: Estimated parameters for the five-parameter Richard’s growth curve (Richards, 1959) for male and female Bigg’s killer whales: average asymptotic adult size (Equation 1, parameter d) and age of inflection (Equation 1, parameter e), as well as their associated standard error.....16
- Table 7: Mean eye patch ratio (EPR, a proxy for body condition, see Fearnbach et al. 2019) and standard deviations associated with each age/sex class of Bigg’s killer whale measured, presented alongside sample size for each class and associated age bracket. Male and female individuals are not treated separately until reaching adulthood, at which point secondary sexual characteristics in males become apparent (Olesiuk et al. 2005; Bigg, 1982; Robeck and Monfort, 2005, Fearnbach et al. 2011) and affect morphology. Post-

reproductive or ‘senescent’ females are treated separately from reproductive-age females, but senescence is not known to occur in male killer whales.....19

Table 8: Mean eye patch ratio (EPR, a proxy for body condition, see Fearnbach et al. 2019) and standard deviation for six age/sex classes of sympatric Bigg’s (this study) and Southern Resident (Stewart et al. 2020) killer whales.....24

ACKNOWLEDGEMENTS

This work would not exist without the support of more people than I can name, though I'll do my best.

I am incredibly grateful for the guidance of my mentors and coworkers at NOAA Southwest Fisheries Science Center, particularly Dave Weller, Tomo Eguchi, Alyssa Paredes, Paige Casler, and Josh Stewart. So too am I indebted to the UCSD faculty members of my advising committee, Simone Baumann-Pickering, John Hildebrand, and Carolyn Kurle, for their patience and insight over the course of this project and beyond. My gratitude also goes to Craig Matkin, Dylan Jones, and Jessica Farrer for assisting John Durban, Holly Fearnbach, and Lance Barrett-Lennard with data collection in the field. To my many wonderful friends (Ana, Nikesh, Ariana, Sarah, and Maddie) for the lightness they bring to years of intense study, and to my parents and sister for their tireless support while I fling myself around the world in pursuit of sea monsters: thank you for enabling my madness.

And most of all I am impossibly grateful to John Durban and Holly Fearnbach for their fierce and unwavering support over the last two years and for teaching me everything I know of photogrammetry and flight. In collaboration with Lance Barrett-Lennard, they gifted me a dataset of which most ecologists cannot even dream. For opening the door to everything that comes next, I'll never be able to say it enough: Thank you, thank you, thank you.

Flights conducted off Northern Vancouver Island, British Columbia, Canada, were authorized by Transport Canada (SFOC 9723488, 10854645 11939499, 13026742) with whale research authorized by Fisheries and Oceans Canada SARA license 2014-06 SARA-327. Flights conducted in the Salish Sea surrounding the San Juan Islands were authorized by an MOU

between the National Ocean and Atmospheric Administration (NOAA) and the Federal Aviation Administration (FAA) and also under FAA part 107 regulations. Whale research was authorized by National Marine Fisheries Service Permits 16163 and 19091.

Funding for field efforts and analysis was provided by the SeaWorld Busch Gardens Conservation Fund, the National Fish and Wildlife Foundation Killer Whale Research and Conservation Program, NOAA Office of Marine and Avian Operations (OMAO), NOAA National Marine Fisheries Service Office of Science and Technology, SR3 Sealife Rehabilitation, Response, and Research, the Vancouver Aquarium, and the National Fish and Wildlife Foundation.

This work is coauthored with John Durban, Holly Fearnbach, Lance Barrett-Lennard, and Chloe Kotik. The thesis author was the primary author of this work and led all image and data analysis.

ABSTRACT OF THE THESIS

Aerial photogrammetry to estimate size, growth, and body condition of mammal-eating Bigg's
killer whales

by

Chloe Kotik

Master of Science in Marine Biology

University of California San Diego, 2020

Simone Baumann-Pickering, Chair

Food availability has been identified as a critical factor influencing the growth, individual health, and population dynamics of killer whales (*Orcinus orca*) in the coastal waters of the

eastern North Pacific Ocean. In investigation of these life history parameters, 113 hand-launched unmanned aerial system flights were conducted over mammal-eating Bigg's killer whales around Vancouver Island between 2014 and 2019, resulting in 20,545 aerial photographs of 95 individually identified animals. I conducted photogrammetric measurements from high-quality images on 91 individuals, a sample that ranged from first-year calves to mature adults of both sexes. Individual lengths ranged from a 2.4m neonate to an 8.3m 38-year-old male. Using a Richard's growth curve model, I estimated asymptotic adult length at 6.4 ± 0.1 m (standard error) in females and 7.3 ± 0.2 m in males, as well as age of inflection at 14.2 ± 2.8 (standard error) years in females and 18.4 ± 2.3 years in males. Comparison with sympatric salmon-eating Southern Resident killer whales found that both sexes of Bigg's killer whale measured significantly longer than Southern Residents (female z-test $P = 0.003$; male z-test $P = 0.093$) but there was no significant difference in age of inflection between males (z-test, $P = 0.53$) or females (z-test, $P = 0.45$) between the two populations. Analysis of eye patch ratio (a proxy for body condition) revealed that all age/sex classes of Bigg's killer whales were more robust than Southern Resident killer whales; the difference was most significant when comparing calves (z-test, $P < 0.0001$) and juveniles (z-test, $P < 0.0001$) between the two populations. I propose that in the absence of major discrepancies in growth trends, morphometric divergences between the two populations are largely a function of prey availability.

Introduction

Analyses of individual size and body condition lend critical insight to the most fundamental aspects of life history. Morphometric data may be used to inform growth trends (Laslett et al. 2004; Fearnbach et al. 2011; Groskreutz et al. 2019), estimate energetic requirements (Bigg and Wolman, 1975; Noren, 2011), and assess health in sensitive populations (Pettis et al. 2004; Miller et al. 2012; Fearnbach et al. 2018; Christiansen et al. 2020). However, assessing body size and condition in wild cetaceans was historically impossible without invasive capture until recent technological advances brought Unmanned Aerial Systems (UAS, colloquially known as ‘drones’) into use. UAS technology is increasingly applied to field research on marine mammals, including population surveys, behavioral observation, photographic identification, and photogrammetry, or the process of obtaining measurements from photographs (Durban et al. 2015a; Fiori et al. 2017).

Although manned aircraft surveys have been utilized in the past for photogrammetry (Perryman and Lynn, 2002; Pitman et al. 2007; Fearnbach et al. 2011; Miller et al. 2012), UAS are significantly smaller, cheaper, and quieter, allowing for lower flights and higher resolution imagery that does not disturb study subjects; they may also be launched from vessels in remote regions not accessible to other aerial platforms (Durban et al. 2015a; Dawson et al. 2017). In combination with photogrammetry, UAS systems provide safe, cost-effective, and powerful investigative tools that are increasingly utilized to monitor the growth and body condition of sensitive cetacean species at sea (Durban et al. 2015a; Durban et al. 2016; Dawson et al. 2017; Fearnbach et al. 2019; Groskreutz et al. 2019; Christiansen et al. 2020; Stewart et al. 2020).

The first application of UAS photogrammetry on cetaceans was to study killer whales (*Orcinus orca*) off Vancouver Island, British Columbia (Durban et al. 2015a). Two distinct

ecotypes of killer whale overlap in these coastal waters: fish-eating ‘Resident’ and mammal-eating ‘Bigg’s’ killer whales (BKWs), formally known as ‘Transient’ killer whales (Bigg, 1982; Barret-Lennard et al. 1996; Ford et al. 1996; Ford et al. 1998; Barrett-Lennard and Ellis, 2001). Though sympatric, the two ecotypes exhibit genetic, acoustic, dietary, behavioral, and reproductive isolation, rendering them ecologically distinct units (Baird and Dill, 1995; Barrett-Lennard et al. 1996; Ford et al. 1998; Baird and Whitehead, 2000; Barrett-Lennard and Ellis, 2001; Moura et al. 2015). Two populations of Resident killer whale occupy the waters surrounding Vancouver Island: “Northern” and “Southern” Residents, which generally aggregate around northern and southern Vancouver Island, respectively (Ford et al. 1996). Particular scientific attention has been paid to the Southern Residents, an endangered subpopulation currently numbering 73 individuals (Center for Whale Research, whaleresearch.com) known to be at risk from limited availability of their primary prey type, Chinook salmon (*Oncorhynchus tshawytscha*). Extensive research has investigated the population dynamics (Ford et al. 2009; Ward et al. 2009), body size (Bigg and Wolman, 1975; Fearnbach et al. 2011), growth trends (Fearnbach et al. 2011), and nutritional health of Southern Resident individuals (Fearnbach et al. 2018, 2019; Stewart et al. 2020). By contrast, there has been no systematic assessment of length-at-age, growth, or body condition in sympatric mammal-eating Bigg’s killer whales.

BKWs are apex predators that exert top-down forcing on marine mammal prey populations throughout the eastern North Pacific Ocean (Barrett-Lennard and Ellis, 2001; Parsons et al. 2013). They feed on pinnipeds and cetaceans, including California and Steller’s sea lions, harbor seals, harbor and Dall’s porpoises, and gray whales (Baird and Dill, 1995; Ford et al. 1998; Saulitis et al. 2000; Barrett-Lennard et al. 2011). Feeding on other high-level marine predators exposes BKWs to extremely high levels of bioaccumulating anthropogenic pollutants

(Ross, 2006) and they have twice been classified as “Threatened” by the Department of Fisheries and Oceans in Canada (DFO, 2007). Despite their high load of contaminants, the BKW population occupying the coastal waters of Southeast Alaska, British Columbia, and Washington State—designated as the ‘West Coast Transients’—has been increasing in abundance by approximately 4% per year since the 1970s (Ford et al. 2007; Towers et al. 2019), displaying high recruitment and low mortality in the same waters where Southern Residents continue to decline (Center for Whale Research, whaleresearch.com; Barrett-Lennard and Ellis, 2001). To date, there have been no studies to assess growth patterns and body condition of BKWs. Our study combined UAS photogrammetry with a long-term photographic identification and life history dataset to estimate measurements of body size, length-at-age, growth trends, and body condition of individuals in the population, and to compare these parameters with endangered Southern Resident killer whales to examine the key factors influencing individual and population health.

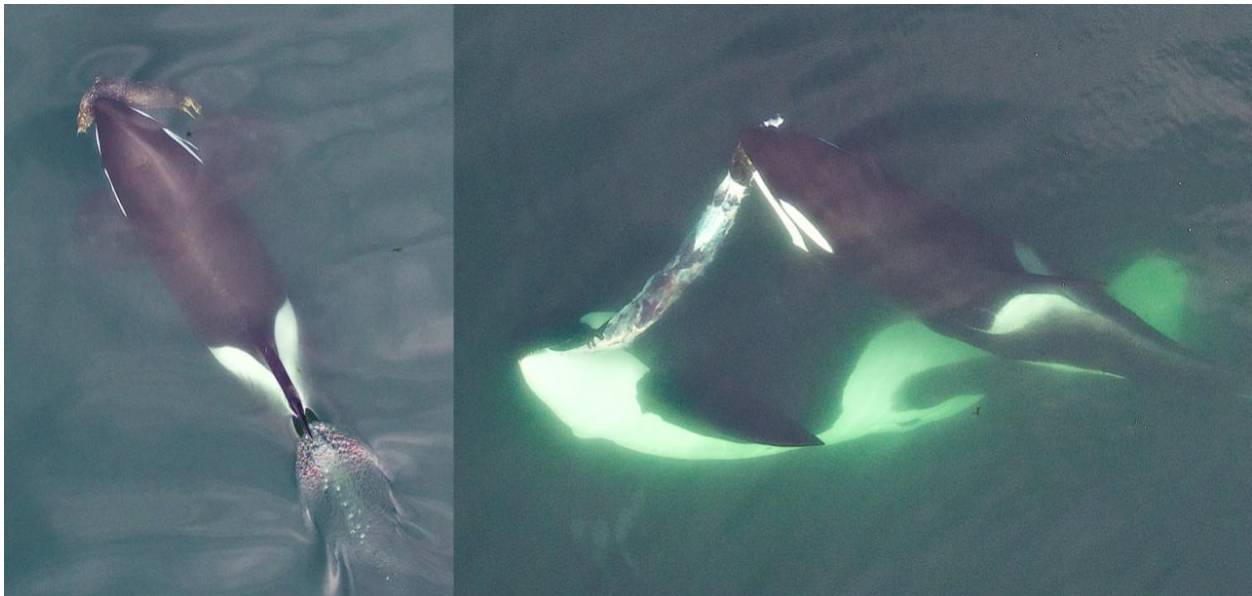


Fig. 1: Aerial images of Bigg’s killer whales. Left: Adult male T123A with a fresh harbor seal kill. Right: Adult male T123A and his mother, T123, sharing a harbor seal kill.

Methods

Aerial photographs of Bigg's killer whales (BKWs) were collected between August 2014 and December 2019 during 14 discrete month-long field efforts, detailed in Table 2. Flights were conducted in two regions: the coastal waters off Northern Vancouver Island, British Columbia, and the Salish Sea region around the San Juan Islands of Washington State (Fig. 1). Between 2014 and 2017, UAS flights were conducted from the upper deck of a 27' fiberglass Sea Sport boat (Durban et al. 2015a), from 2018 to September 2019 flights were conducted from a 31' aluminum catamaran (Fig. 3), and in November 2019 flights were conducted from a 24' rigid-hulled inflatable boat. Six aircraft of two different models were flown (Table 2): the 22" wingspan Aerial Photographic Hexacopter (APH-22) and the 42" wingspan Aerial Photographic Octocopter (APO-42), both from Aerial Imaging Solutions. Both UAS were equipped with mirrorless digital cameras capturing vertical images with Normal lenses that ensured flat images with no wide-angle distortion and water-level pixel resolution of 2cm or better (Durban et al. 2015a). Prior to 2017, the altitude of the aircraft was recorded at 1-second intervals by an onboard pressure altimeter (Durban et al. 2015a); beginning in 2017 a more precise laser altimeter was used (Dawson et al. 2017).

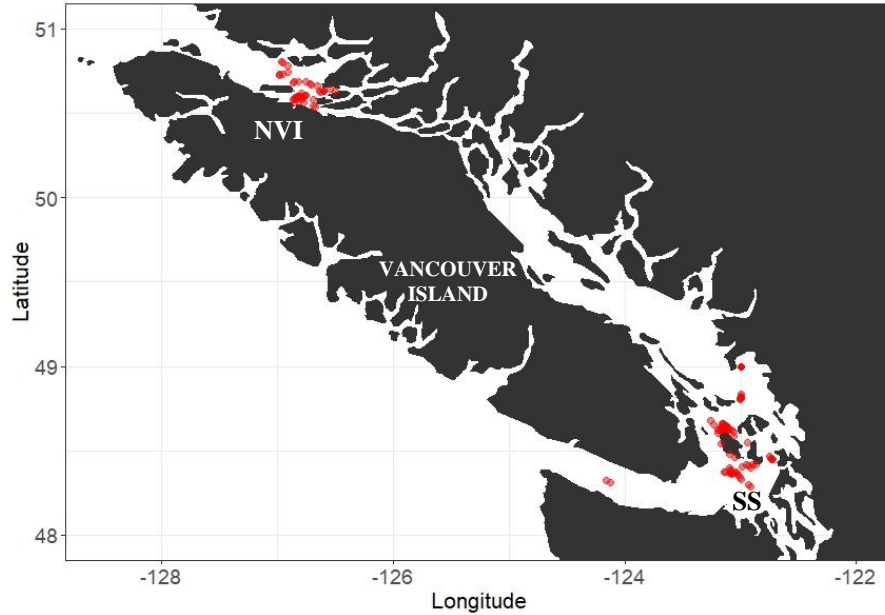


Fig. 2: Locations of 111 flights over Bigg’s killer whales using unmanned aerial systems in the coastal waters off Northern Vancouver Island (NVI), British Columbia, and the Salish Sea (SS) surrounding the San Juan Islands of Washington State.



Fig. 3: John Durban piloting the APO-42 Octocopter (Aerial Imaging Solutions) into the hands of Holly Fearnbach for safe retrieval onboard the R/V *Kohala*. Photo taken by John Calambokidis of the Cascadia Research Collective.

Each aerial image was examined by the author (CK) on a 27-inch high-definition LED flat panel monitor using the ACDSee photo manager program. Photographed Bigg's killer whales were matched to preexisting identifications in an established photographic catalog (Towers et al. 2019) via congenital saddle patch pigmentation and acquired scar patterns (Fig. 4). Whale identifications were corroborated, where possible, using full-color boat-based images collected and published in the Center for Whale Research's 2016 photo identification catalog (Center for Whale Research, 2016) of frequently photographed individuals. All photographs of identified BKWs were subsequently assessed for measurement quality: only photographs depicting animals in flat and elongate surfacing orientation were selected to ensure the highest quality of measurements (Fig. 4). High-quality images of each individual's saddle patch region were selected separately and compiled into an aerial master catalog for future reference.



Fig. 4: Comparison of saddle pigmentation and scarring patterns used to identify adult female T100 in an aerial image (left) compared to left- and right-side boat-based photo-identification images (Towers et al. 2019).

Prior to measurement, high-quality images were rechecked against the 2019 catalog (Towers et al. 2019) and the author's aerial master catalog to ensure correct identification. Using the freely-available image processing program ImageJ (<https://imagej.nih.gov/ij/>), I generated pixel-length measurements of six metrics (Table 1, Fig. 5). To maximize the number of length estimates for BKWs (given that their steep surfacing angle does not typically allow for a single measurement of total length) I collected two separate measurements of length: a snout to dorsal fin (SNDF) measurement from the tip of the rostrum to the anterior insertion of the dorsal fin and a dorsal fin to fluke (DFFL) measurement from the anterior insertion of the dorsal fin to the central margin of the fluke notch (Fig. 5); these measurements were typically from separate but sequential images as each respective body segment was flat and parallel to the water's surface. Total length (TL) estimates were then derived from the addition of maximum SNDF and DFFL values of an individual within a given sampling period, as this could be assumed to represent the flattest description of an individual (Groskreutz et al. 2019). To estimate body condition, I quantified fatness behind the cranium using the eye patch ratio metric developed by Fearnbach et al. (2019), construed from two measurements: eye patch top (EP TOP), a width taken from the inner anterior margin of the right eye patch to the inner anterior margin of the left eye patch, and eye patch bottom (EP BOTTOM), a width taken from the inner margin of the right eye patch at 75% the vertical length of the patch to the inner margin of the left eye patch (Table 1, Fig. 5). Eye patch ratio was derived by dividing EP BOTTOM by EP TOP (Fearnbach et al. 2019) to give a unitless quantification of robustness. EPR is a powerful metric to assess body condition in killer whales, which are vulnerable to the loss of adipose tissue behind the head when subjected to nutritional stress. Higher EPR values indicate more robust individuals (Fearnbach et al. 2019).

Table 1: Detailed descriptions of each photogrammetry measurement. Measurements in pixels were conducted in ImageJ and subsequently converted to real length estimates.

Measurement	Description
Snout to dorsal fin (SNDF)	Tip of rostrum to anterior insertion of dorsal fin
Dorsal fin to fluke (DFFL)	Anterior insertion of dorsal fin to central margin of fluke notch
Total length (TL)	Derived as SNDF + DFFL
Eye patch top (EP TOP)	Horizontal distance between interior margins of eye patches at the anterior end of the patches
Eye patch bottom (EP BOTTOM)	Horizontal distance between interior margins of eye patches, at 75% to the caudal limits of the eye patches
Eye patch ratio (EPR)	Derived as EP BOTTOM / EP TOP

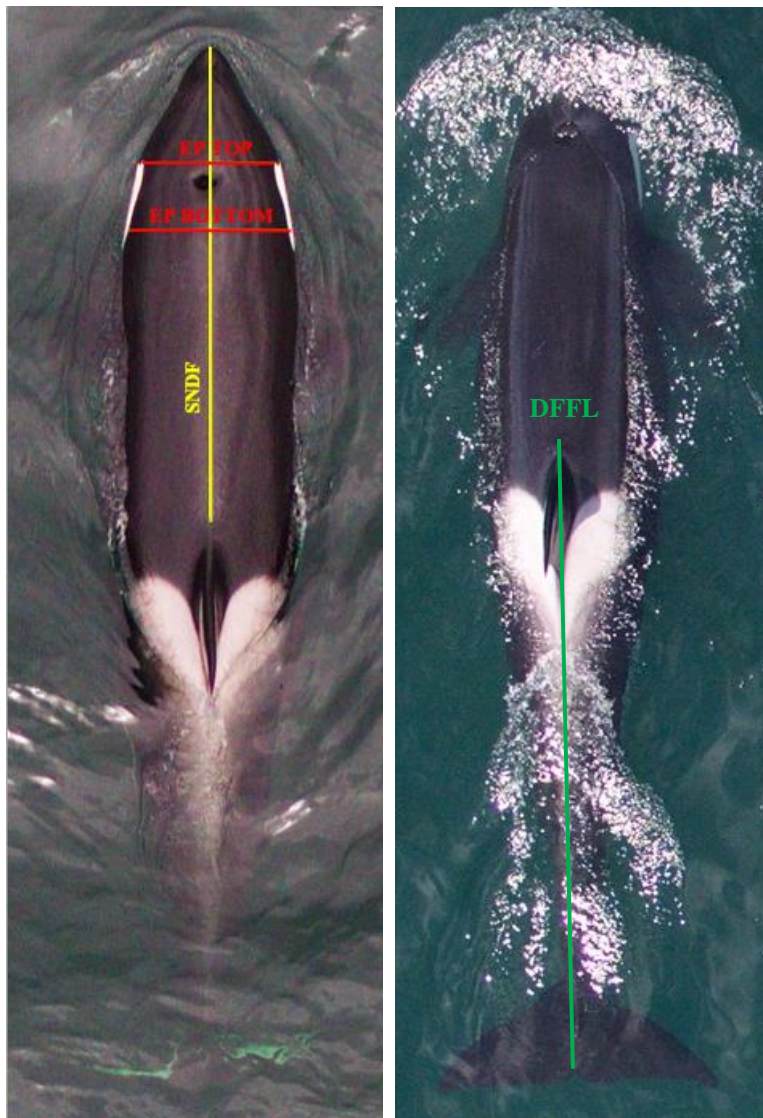


Fig. 5: Aerial images of Bigg's killer whales showing pixel length measurements conducted in ImageJ on BKW T124A2. Left: upper and lower eye patch measurements (EP TOP and EP BOTTOM, in red) and snout to dorsal insertion (SNDF, in yellow). Right: dorsal insertion to fluke notch (DFFL, in green).

All pixel measurements of length were scaled to real length estimates using their ratio to the known size of the camera sensor (i.e. 4608 pixels = 17.3mm wide) and were then scaled using the known altitude of the UAS (collected at the time of capture by an onboard laser altimeter) and the realized lens focal length (scale = altitude / focal length). The average growth trends of BKWs were then estimated by fitting the Richard's growth curve model (Richards, 1959) to length-at-age data of males and females separately (Fearnbach et al. 2011). Ages of individual BKWs were determined from the birth years provided in the most recent population identification catalog (Towers et al. 2019), encompassing over 60 years of birth and sighting records. Ages were standardized by setting all birth dates to February 1 in the first year of life based on the established calving trends of Resident killer whales, with whom BKWs share many aspects of life history (Ford and Ellis, 1999; Olesiuk et al. 2005; Towers et al. 2019). Individual sex was also reported by Towers et al. (2019) and determined by the visual identification of secondary sexual characteristics in males (dorsal fin elongation and enlarged pectoral fins), genital pigmentation patterns, or the birth of a calf (Towers et al. 2019). Additionally, the sexes of 4 younger animals were determined for the first time based on genital pigmentation patterns documented in our aerial images.

In cases where animals were encountered more than once across the study period, length data (SNDF, DFFL, and TL) were taken from the most recent sampling period so each individual would only be represented once in the growth curve; this also preferentially selected later measurements that were associated with laser rather than pressure altimetry, as the error associated with the pressure altimeter (<1%) exceeds that associated with the laser (0.1%) (Durban et al. 2015a; Dawson et al. 2017). Given that length measurement variability is largely attributed to foreshortening of whales imaged when not elongating to maximum length

(Fearnbach et al. 2011), I further selected the maximum values associated with each length metric (SNDF and DFFL) for each individual in each sampling period.

The Richard's growth curve (Equation 1) describes length-at-age (L) as a function of asymptotic adult length (d), age in years (t), the position of the inflection point relative to the asymptote (e), and free parameters adjusting the slope and inflection point (b , c , and f) (Richards, 1959). The standard R statistical package was used to apply non-linear least square model fitting of the Richard's curve.

$$L = c + \left(\frac{d - c}{1 + \exp(b(\log(t)) - \log(e))} \right)^f$$

Equation 1: The five-parameter Richard's growth curve equation describing the relationship between total body length L , asymptotic adult size d , age in years t , inflection point e , and freely adjusting parameters b , c , and f (Richards, 1959).

In assessment of body condition, I calculated the mean EPR for each whale in each sampling period. EPR provides a consistent and powerful measure of body condition with low measurement variability for an individual in a sampling period (typical coefficient of variation = standard deviation/mean of <1%) (Fearnbach et al. 2019). Consequently, small seasonal or yearly changes are readily detected within the EPR and are indicative of long-term health trends (Fearnbach et al. 2019; Stewart et al. 2020). Measured individuals were divided into the following age and sex classes based on reproductive and growth trends established herein as well as those already known (Olesiuk et al. 2005; Fearnbach et al. 2011; Towers et al. 2019): calf (0-3 years old), juvenile (3-10 years old), subadult (10-15 years old), adult female (15-45 years old), adult male (15+ years), and senescent female (45+ years old). Eye patch ratio was calculated not as a maximum value, but as an average; while length-based metrics are negatively biased by

foreshortening and failure to elongate fully during surfacing, relative width measurements are affected by the degree of flexion in the individual and are therefore best represented by average values, both within individuals and entire age/sex classes. Some whales were sighted during multiple sampling periods; their measurements may be included in multiple age class summaries reflecting their growth over time.

Results

A total of 113 UAS survey flights were conducted over BKWs from 2014 to 2019 in the coastal waters off Northern Vancouver Island (NVI) and the Salish Sea region (SS). Average flight duration for the entire effort was 12.2 minutes (max = 24.1 min); average altitude was 36.9m (121.1 ft). In total, 19.7 hours were spent in flight from 2014 to 2019.

Table 2: Detailed metrics regarding the year, month, location, duration, and altitude of UAS flights conducted over Bigg’s killer whales in two main regions: the coastal waters of Northern Vancouver Island (NVI), British Columbia, and the Salish Sea (SS) surrounding the San Juan Islands of Washington. Two flights conducted in May of 2018 did not yield duration, altitude, or location data.

Year	Month	Location	Number of Flights	Whale IDs	Total Flight Time (min)	Avg. Flight Duration (min)	Avg. Max Altitude (m)	UAS
2014	8	NVI	3	6	39.38	13.13	36.73	APH22-11
2015	8	NVI	21	21	218.47	10.40	39.52	APH22-11
2015	9	SS	1	6	9.92	9.92	40.09	APH22-12
2016	5	SS	20	22	258.57	12.93	43.30	APH22-12
2016	8	NVI	8	16	101.07	12.63	36.08	APH22-13
2016	9	SS	4	7	42.52	10.63	37.43	APH22-11
2017	5	SS	10	10	92.93	9.29	33.44	APH22-19
2017	8	NVI	9	15	101.73	11.30	33.21	APH22-11
2017	9	SS	7	12	69.27	9.90	32.96	APH22-11
2018	5	SS	10	29	169.25	16.93	38.60	APO42_01
2018	9	SS	1	5	23.75	23.75	36.20	APO42_01
2019	5	SS	2	8	33.017	16.51	38.34	APO42_01
2019	9	SS	1	4	23.32	23.32	43.69	APO42_41

These UAS flights resulted in 20,545 aerial photographs of Bigg's killer whales. Of these, 1,651 were deemed of high enough quality for measurement for an identified individual whale, from which 8,930 measurements were generated in ImageJ. A total of 95 individual BKWs were identified from aerial images and catalogued during our surveys; 91 were photographed in orientation and quality suitable for measurement. Nearly half (41) of the animals were imaged during multiple sampling periods across the study.

Of the 95 sampled individuals, SNDF and DFFL measurements were available from flat images for 86 whales (39 estimated using pressure altimetry data, 47 using laser altimetry data). Sex was linked to 67 of the measured individuals (Towers et al. 2019). SNDF and DFFL measurements were typically conducted multiple times: average # of SNDF measurements per animal = 6.3, median = 6, range 1-18; average # of DFFL measurements per animal = 3.4, median = 2, range = 1-13.

In confirmed females, total length estimates ranged from 2.4m for a first-year calf (T65A6) to 7.1m for a 33-year-old (T123); in confirmed males, TL ranged from 4.8m for a four-year-old (T49A4) to 8.3m for a 38-year-old (T11A). Individuals of unknown sex were typically younger and smaller (photographed prior to the development of sexually diagnostic characteristics at the onset of maturity) and ranged from 2.9m (first-year calf T75B2) to 5.7m (11-year-old T65A3).

Table 3: Whale ID, year and month of capture, sex, altimeter, age, maximum total length (TL), and number of measures for snout to dorsal fin insertion (SNDF) and dorsal fin insertion to fluke (DFFL) of 41 confirmed female Bigg’s killer whales, all taken from the most recent sampling period for each individual. Maximum TL was derived by combining the maximum SNDF and DFFL values measured within a sampling period.

Whale ID	Year	Month	Sex	Altimeter Type	Age (years)	Maximum TL (m)	# Measures (SNDF)	# Measures (DFFL)
T65A6	2018	6	F	Laser	0.3	2.4	6	5
T124A2B	2017	5	F	Laser	1.3	4.0	2	2
T49A5	2018	6	F	Laser	1.3	3.4	4	1
T86A4	2018	5	F	Laser	2.3	4.1	2	1
T60F	2015	8	F	Pressure	3.5	4.0	2	1
T36A2	2016	5	F	Pressure	4.3	4.2	3	2
T123C	2018	5	F	Laser	6.3	4.9	11	7
T86A3	2018	5	F	Laser	7.3	5.0	3	1
T65A4	2018	6	F	Laser	7.3	4.9	15	2
T90C	2019	5	F	Laser	9.3	5.6	7	2
T137B	2016	8	F	Pressure	10.6	5.9	5	6
T100E	2019	9	F	Laser	10.6	5.4	6	3
T36A1	2016	5	F	Pressure	11.3	6.0	5	1
T124A3	2017	5	F	Laser	11.3	5.9	11	7
T69D	2015	8	F	Pressure	14.5	5.9	1	2
T124A2	2019	5	F	Laser	18.3	6.4	11	3
T59A	2015	8	F	Pressure	20.5	5.7	7	1
T75B	2015	9	F	Pressure	20.6	5.5	4	2
T124A1	2017	5	F	Laser	21.3	6.6	10	8
T65B	2017	9	F	Laser	24.6	6.4	7	3
T49B	2017	9	F	Laser	25.7	6.5	3	3
T36A	2016	5	F	Pressure	26.3	6.1	12	8
T41A	2016	8	F	Pressure	28.6	6.9	2	2
T69A	2017	8	F	Laser	28.6	6.3	11	9
T86A	2018	5	F	Laser	30.4	6.3	7	2
T99	2016	5	F	Pressure	32.3	6.4	9	2
T65A	2018	6	F	Laser	32.4	6.7	18	2
T49A	2018	6	F	Laser	32.4	6.4	5	2
T137	2016	8	F	Pressure	32.6	6.1	8	6
T123	2018	5	F	Laser	33.3	7.1	7	5
T124A	2017	5	F	Laser	33.3	6.6	14	9
T7B	2016	8	F	Pressure	34.6	6.1	9	3
T2B	2014	8	F	Pressure	35.6	6.6	3	3
T60	2016	9	F	Pressure	36.6	6.0	8	6
T90	2019	5	F	Laser	39.3	6.8	10	3
T58	2015	8	F	Pressure	39.6	5.5	6	2
T100	2019	9	F	Laser	40.7	6.3	3	2
T69	2017	8	F	Laser	43.6	6.7	12	2
T59	2015	8	F	Pressure	45.6	6.1	5	2
T11	2016	5	F	Pressure	52.3	6.3	8	6
T10	2016	8	F	Pressure	52.6	6.0	2	2

Table 4: Whale ID, year and month of capture, sex, altimeter, age, maximum total length (TL), and number of measures for snout to dorsal fin insertion (SNDF) and dorsal fin insertion to fluke (DFFL) of 26 confirmed male Bigg’s killer whales, all taken from the most recent sampling period for each individual. Maximum TL was derived by combining the maximum SNDF and DFFL values measured within a sampling period.

Whale ID	Year	Month	Sex	Altimeter Type	Age (years)	Maximum TL (m)	# Measures (SNDF)	# Measures (DFFL)
T49A4	2018	6	M	Laser	4.3	4.8	6	4
T65A5	2018	6	M	Laser	4.3	4.7	3	2
T65B1	2016	5	M	Pressure	5.3	4.2	4	1
T124A2A	2019	5	M	Laser	6.3	5.0	10	2
T49A3	2018	6	M	Laser	7.3	5.6	5	2
T60E	2016	9	M	Pressure	8.6	4.3	7	5
T49A2	2018	6	M	Laser	11.3	5.8	7	3
T7B3	2016	8	M	Pressure	11.5	6.3	6	1
T69A2	2017	8	M	Laser	11.6	5.6	2	2
T60D	2016	9	M	Pressure	12.6	4.5	11	7
T90B	2018	9	M	Laser	12.6	7.0	10	4
T60C	2014	8	M	Pressure	13.6	7.4	4	1
T65A2	2018	6	M	Laser	14.3	7.0	10	5
T137A	2016	8	M	Pressure	14.6	6.5	2	2
T10C	2015	8	M	Pressure	16.5	6.7	8	5
T49A1	2018	6	M	Laser	17.3	7.1	4	1
T100C	2019	9	M	Laser	17.6	7.2	2	2
T123A	2018	5	M	Laser	18.3	7.5	11	1
T77A	2017	5	M	Laser	21.3	7.2	3	2
T101A	2018	5	M	Laser	25.3	7.6	4	2
T10B	2015	8	M	Pressure	32.5	6.7	6	1
T97	2016	5	M	Pressure	36.3	6.3	8	3
T11A	2016	5	M	Pressure	38.3	8.3	12	3
T54	2015	8	M	Pressure	43.6	7.4	8	3
T93	2016	5	M	Pressure	52.3	7.5	11	1
T87	2019	5	M	Laser	57.3	7.1	3	2

Table 5: Whale ID, year and month of capture, sex, altimeter, age, maximum total length (TL), and number of measures for snout to dorsal fin insertion (SNDF) and dorsal fin insertion to fluke (DFFL) for 19 Bigg’s killer whales of unknown sex, all taken from the most recent sampling period for each individual. Maximum TL was derived by combining the maximum SNDF and DFFL values measured within a sampling period.

Whale ID	Year	Month	Sex	Altimeter Type	Age (years)	Maximum TL (m)	# Measures (SNDF)	# Measures (DFFL)
T75B2	2015	9	U	Pressure	0.6	2.9	2	2
T99D	2016	5	U	Pressure	1.3	3.8	4	1
T69A4	2017	8	U	Laser	1.6	3.8	6	10
T7B5	2016	8	U	Pressure	2.1	3.9	7	6
T90D	2019	5	U	Laser	2.3	4.1	4	5
T59A3	2015	8	U	Pressure	2.5	3.5	3	1
T100F	2018	5	U	Laser	4.3	3.9	5	5
T137D	2016	8	U	Pressure	4.6	4.2	7	5
T49B3	2017	9	U	Laser	4.6	4.2	2	3
T59A2	2015	8	U	Pressure	6.5	3.9	3	3
T7B4	2016	8	U	Pressure	6.5	4.8	4	2
T69A3	2017	8	U	Laser	6.6	4.6	6	1
T124A4	2017	5	U	Laser	7.3	5.3	12	13
T69F	2017	8	U	Laser	7.6	5.4	3	1
T49B2	2017	9	U	Laser	7.6	4.7	2	2
T99B	2016	5	U	Pressure	9.3	4.6	2	6
T59A1	2015	8	U	Pressure	9.5	5.0	9	5
T65A3	2018	6	U	Laser	11.3	5.7	3	3
T69E	2017	8	U	Laser	13.6	5.5	10	8

Adult female BKWs (ages 15+) ranged from 5.5 to 7.1m (n = 26, mean = 6.3m, median = 6.4m) and adult male BKWs (ages 15+) ranged from 6.3 to 8.3m (n = 12, mean = 7.2m, median = 7.2). The fitted Richard's growth curve (Equation 1) estimated asymptotic adult sizes of 6.4m (SE 0.10) in female and 7.3m (SE 0.22) in male BKWs (Table 6, Fig. 6). These were significantly different from one another (z-test, $P < 0.0001$). By contrast, sympatric fish-eating Southern Resident killer whale females only reach asymptotic adult size of 6.0m (SE 0.08), and 6.9m (SE 0.20) in males (Fearnbach et al. 2011). The asymptotic sizes for both sexes of BKWs were significantly longer than SRKWs (female z-test, $P = 0.003$; male z-test, $P = 0.093$).

Asymptotic growth was reached later in BKW males compared to females; our model found points of inflection (at which growth begins to slow) at 14.2 years (SE 2.77) in females and 18.4 years (SE 2.25) in males (Table 6, Fig. 6) (z-test, $P = 0.12$). These estimates are consistent with established growth trends for SRKWs (Olesiuk et al. 2005; Fearnbach et al. 2011); comparison of growth parameters for SRKWs found no significant difference in age of inflection of males (z-test, $P = 0.53$) or females (z-test, $P = 0.45$) between the two populations. Additionally, calculated TL in the youngest BKW measured (2.4m in 0.3-year-old neonate T65A6) was consistent with estimates of neonate length in SRKWs (2.7m in 0.5-year-old neonate reported in Fearnbach et al. 2011).

Table 6: Estimated parameters for the five-parameter Richard's growth curve (Richards, 1959) for male and female Bigg's killer whales: average asymptotic adult size (Equation 1, parameter d) and age of inflection (Equation 1, parameter e), as well as their associated standard error.

	Asymptotic adult size (m)	Standard error	Age of inflection (years)	Standard error
Females	6.4	0.10	14.2	2.77
Males	7.3	0.22	18.4	2.25

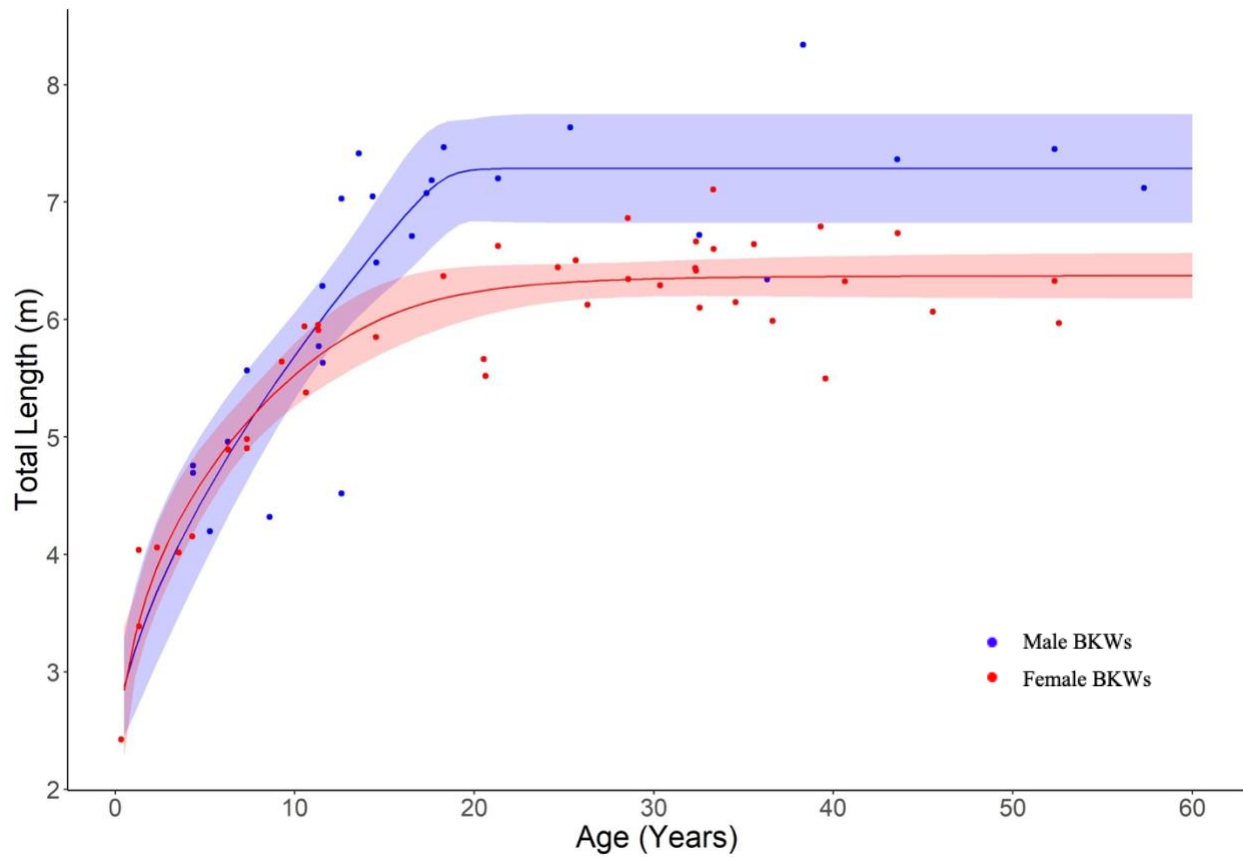


Fig. 6: Total length (TL, in meters) estimates of 41 confirmed female (red) and 26 confirmed male (blue) Bigg’s killer whales plotted against known age of individual. The fitted Richard’s growth curves (Equation 1) are plotted for each sex (females in red, males in blue), the parameters of which are described in Table 6, as well as 95% confidence intervals for the model fit.

I conducted measurements of eye patch ratio (EPR, see Table 1 and Fig. 5) in 91 Bigg's killer whales: 44 females, 31 males, and 16 of unknown sex. Of these, 37 individuals were measured over multiple years. Female calves (ages 0-3) had an average EPR of 1.25 ± 0.03 (SD), female juveniles (ages 3-10) averaged 1.20 ± 0.03 , female subadults (ages 10-15) averaged 1.19 ± 0.02 , female adults (ages 15-45) averaged 1.24 ± 0.05 , and senescent females averaged 1.23 ± 0.03 . Male calves (ages 0-3) had an average EPR of 1.22 ± 0.04 (SD), male juveniles (ages 3-10) averaged 1.19 ± 0.05 , male subadults (ages 10-15) averaged 1.21 ± 0.06 , and male adults (ages 15+) averaged 1.27 ± 0.04 . Calves of unknown sex (ages 0-3) had an average EPR of 1.20 ± 0.05 (SD), juveniles of unknown sex (ages 3-10) averaged 1.17 ± 0.04 , and subadults of unknown (ages 10-15) averaged 1.20 ± 0.03 . No older animals of unknown sex were imaged, as mature male killer whales present with diagnostic sexual characteristics.

There was a significant difference in the EPR values of BKWs of different age/sex classes (ANOVA, $P < 0.0001$). While initially born at relatively robust EPR values (mean $1.22 \pm$ SD 0.04), BKWs experienced a 'juvenile slump' in EPR when growing through juvenile and subadult stages (1.19 ± 0.04 in juveniles and 1.20 ± 0.04 in subadults) persisting up to sexual maturity, at which point male BKWs measured notably higher in EPR than adult females (1.27 ± 0.04 in adult males compared to 1.24 ± 0.05 in adult females), including senescent females (1.23 ± 0.04) (Table 7).

Table 7: Mean eye patch ratio (EPR, a proxy for body condition, see Fearnbach et al. 2019) and standard deviations associated with each age/sex class of Bigg’s killer whale measured, presented alongside sample size for each class and associated age bracket. Male and female individuals are not treated separately until reaching adulthood, at which point secondary sexual characteristics in males become apparent (Olesiuk et al. 2005; Bigg, 1982; Robeck and Monfort, 2005, Fearnbach et al. 2011) and affect morphology. Post-reproductive or ‘senescent’ females are treated separately from reproductive-age females, but senescence is not known to occur in male killer whales.

Class	Age bracket (years)	# Individuals	Average EPR	SD
Calf	0-3	17	1.22	0.04
Juvenile	3-10	44	1.19	0.04
Subadult	10-15	22	1.20	0.04
Adult female	15-45	42	1.24	0.05
Adult male	15+	23	1.27	0.04
Senescent female	45+	5	1.23	0.03

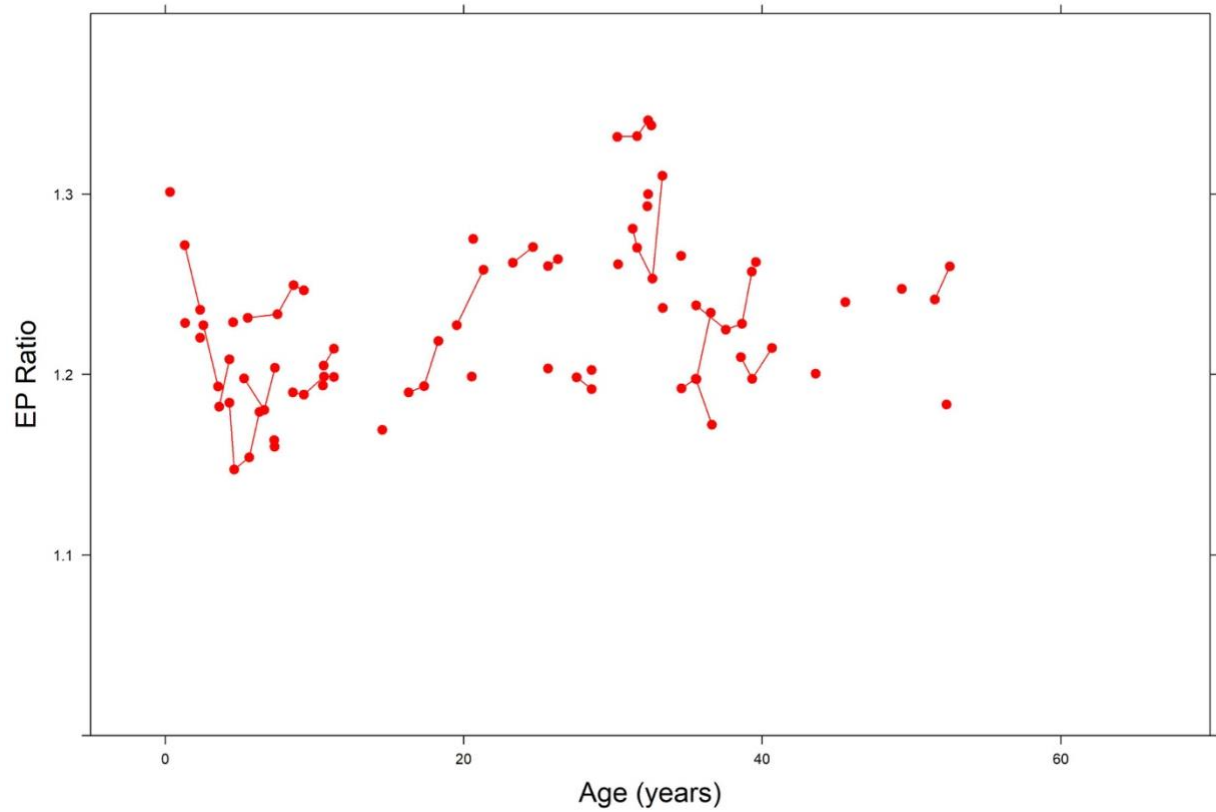


Fig. 7: Eye patch ratio (EPR, a proxy for body condition) values for 44 confirmed female Bigg's killer whales ranging in age from 0.3 to 52.6 years. Points represent the average values of each individual in each sampling period. Lines represent repeat measurements of the same individual across sampling periods.

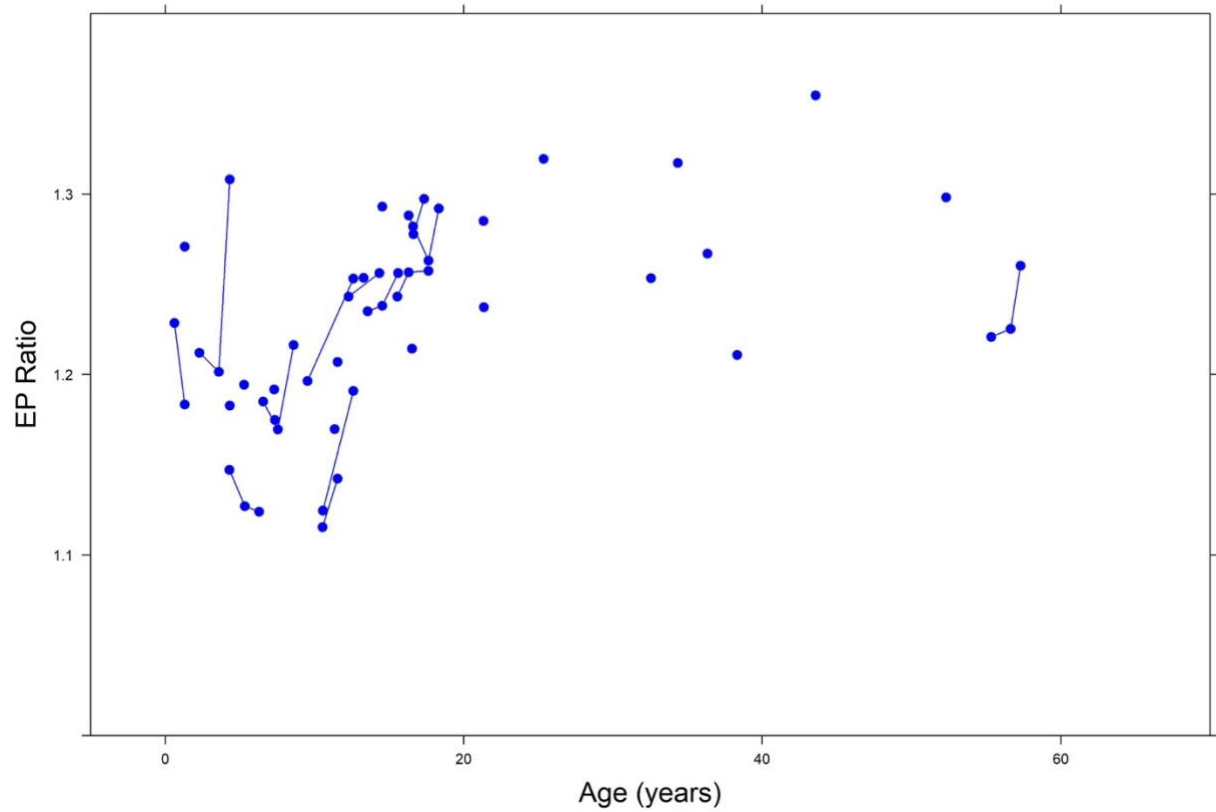


Fig. 8: Eye patch ratio (EPR, a proxy for body condition) values of 31 confirmed male Bigg's killer whales ranging in age from 0.6 to 57.3 years. Points represent the average values of each individual in each sampling period. Lines represent repeat measurements of the same individual across sampling periods.

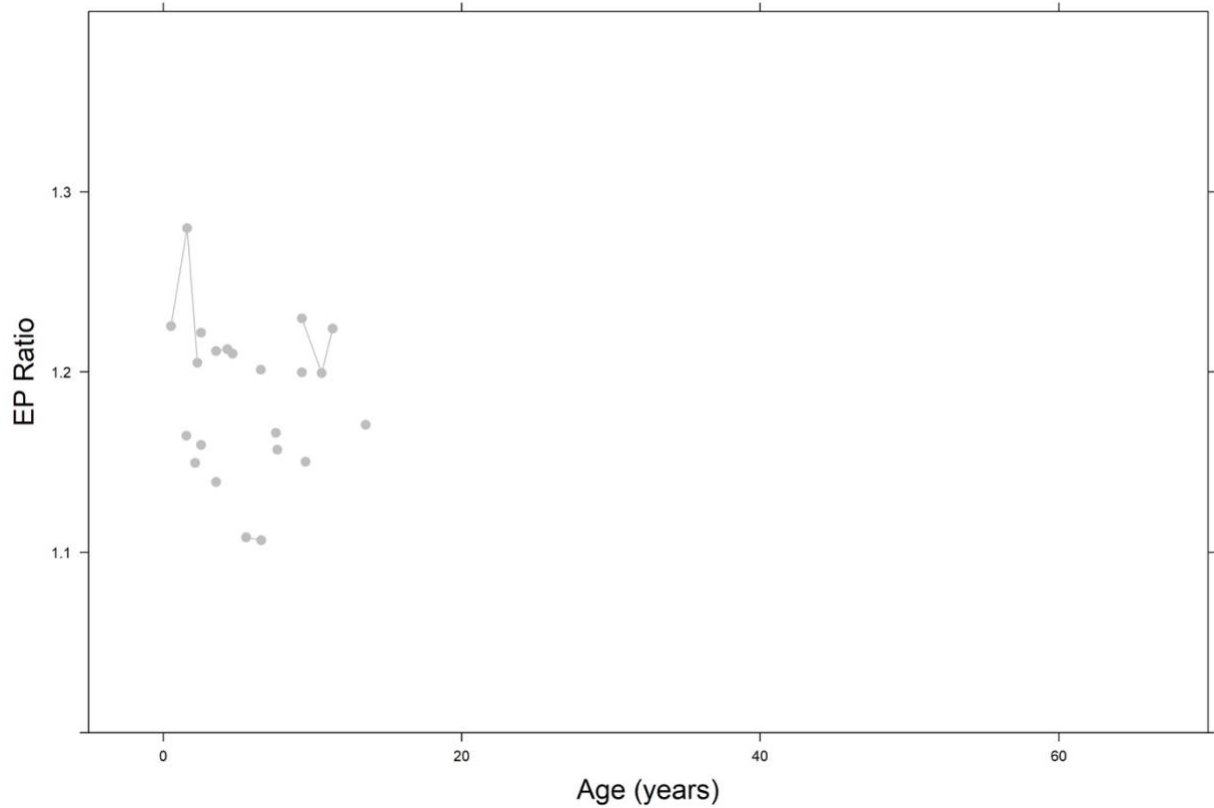


Fig. 9: Eye patch ratio (EPR, a proxy for body condition) values of 16 Bigg’s killer whales of unknown sex ranging in age from 0.5 to 13.6 years. Points represent the average values of each individual in each sampling period. Lines represent repeat measurements of the same individual across sampling periods.

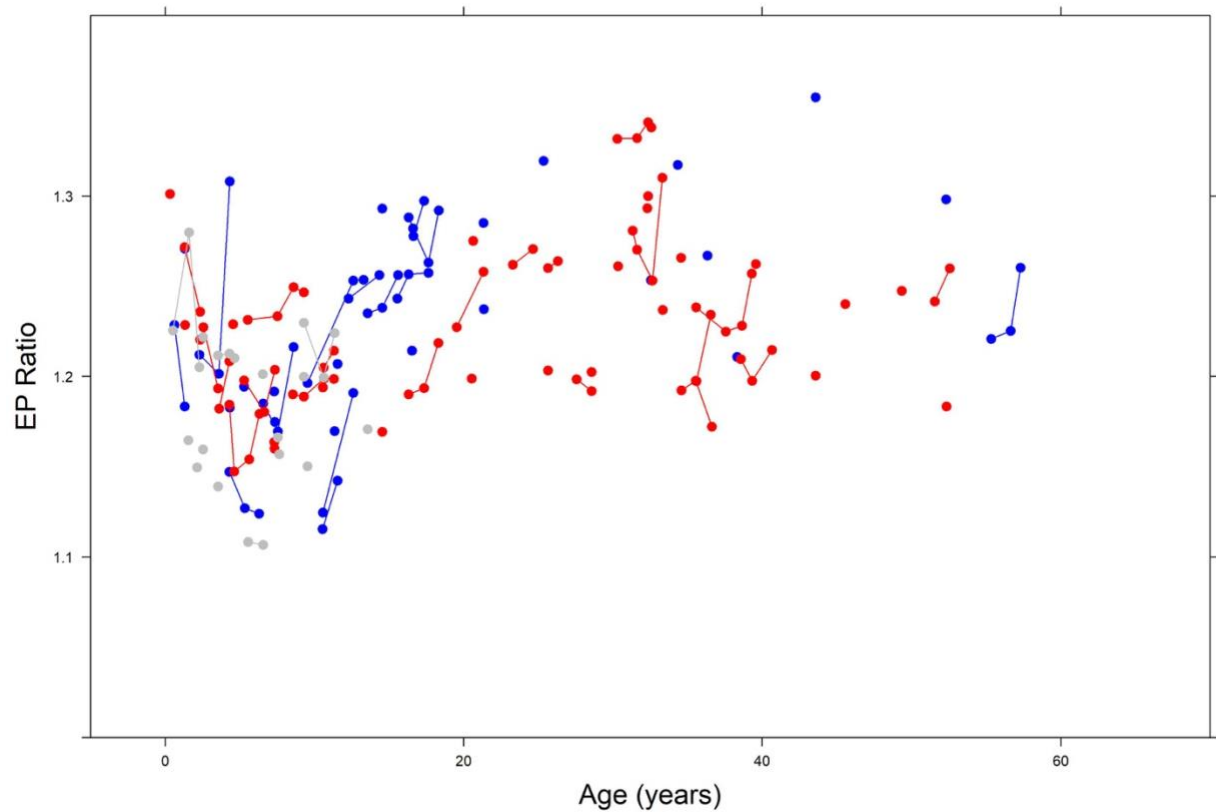


Fig. 10: Eye patch ratios (EPR, a proxy for body condition) of 91 individual Bigg’s killer whales: 44 females (ranging in age from 0.3 to 52.6 years, in red), 31 males (ranging in age from 0.6 to 57.3 years, in blue), and 16 of unknown sex (ranging in age from 0.5 to 13.6 years, in gray). Points represent the average values of each individual in each sampling period. Lines represent repeat measurements of the same individual across sampling periods.

Comparison of EPR values between BKWs and sympatric fish-eating SRKWs found higher mean EPR values in all classes of BKWs, and the difference was most significant when comparing calves (z-test, $P < 0.0001$) and juveniles (z-test, $P < 0.0001$) between the two populations. Adult male BKWs were still significantly more robust than adult male SRKWs (z-test, $P = 0.0015$), as were senescent female BKWs compared to senescent female SRKWs (z-test, $P = 0.0560$), but the trend was weakest when comparing subadults (z-test, $P = 0.1520$) and adult females (z-test, $P = 0.1003$) between the two populations.

Table 8: Mean eye patch ratio (EPR, a proxy for body condition, see Fearnbach et al. 2019) and standard deviation for six age/sex classes of sympatric Bigg’s (this study) and Southern Resident (Stewart et al. 2020) killer whales.

Class	Age bracket (years)	# Bigg’s sampled	Bigg’s mean EPR	Bigg’s SD	# SRKW sampled	SRKW mean EPR	SRKW SD
Calf	0-3	17	1.22	0.04	29	1.16	0.04
Juvenile	3-10	44	1.19	0.04	98	1.15	0.03
Subadult	10-15	22	1.20	0.04	161	1.19	0.04
Adult female	15-45	42	1.24	0.05	83	1.23	0.03
Adult male	15-45	23	1.27	0.04	22	1.24	0.03
Senescent female	45+	5	1.23	0.03	80	1.21	0.04

Discussion

This is the first study estimating size, growth, and body condition of Bigg's killer whales. Prior to this work, length estimates for BKWs in a live-capture fishery had not been separated from those of captured Resident killer whales (Bigg and Wolman, 1975); likewise, body condition had not been systematically assessed. I utilized a unique preexisting dataset of aerial images collected using non-invasive, low-impact UAS to identify and conduct morphometric photogrammetry upon 95 individual BKWs. This sample represents over 27% of the known population of coastal West Coast Transients (Towers et al. 2019) and sampled individuals ranged in age from newborn calves to mature adults of both sexes, representing all age/sex classes between and allowing for thorough investigation into the life history underpinnings of morphometry.

In the last twenty years, BKWs have twice been classified as "Threatened" under the Species at Risk Act (SARA) by the Department of Fisheries and Oceans in Canada (DFO, 2007). They are affected by the same anthropogenic pressures facing sympatric marine mammals (e.g. varying prey availability, habitat loss and disruption, and acoustic and physical disturbances), but as high-level trophic predators, BKWs are particularly vulnerable to persistent bioaccumulating toxins (PBTs). Among these, polychlorinated biphenyls (PCBs) and polybrominated diphenyl ethers (PBDEs) occur at potentially dangerous levels in Bigg's killer whales (Ross and Ellis, 2000; Ross, 2006). In spite of toxic accumulation and other mounting pressures, the abundances of BKWs have been increasing since the 1970s as a function of low mortality and high recruitment (Ford et al. 2007). In contrast, the sympatric Southern Resident killer whale population has been declining in abundance since the 1990s (Ward et al. 2009), dropping to only 73 individuals as of December 31, 2019 (Center for Whale Research, whaleresearch.com). The

analysis herein estimates that growth trends in BKWs are highly consistent with those in SRKWs: the total lengths of the youngest neonates measured were consistent between 2-3m (Table 3 and Fearnbach et al. 2011), age of inflection (slowed growth) between BKWs and SRKWs was consistent in both males (z-test, $P = 0.53$) and females (z-test, $P = 0.45$) (Table 6 and Fearnbach et al. 2011), and the ‘juvenile slump’ phenomenon detected in Bigg’s killer whales has also been established in SRKWs (Fearnbach et al. 2018). However, BKWs were estimated to be longer and more robust than SRKWs, which only reach maximum lengths of 6.4m in adult females and 7.2m in adult males (Fearnbach et al. 2011), while adult female BKWs reached up to 7.1m and adult male BKWs reached 8.3m. Notably, the length-weight relationship in killer whales is not linear: a 7.3m animal (the asymptotic adult length of a male BKW) weighs approximately 670 pounds more than a 6.9m animal (the asymptotic adult length of a male SRKW) (Bigg and Wolman, 1975). Even these calculations were based on undifferentiated measurements of Resident and Bigg’s killer whales from a live-capture fishery, and do not account for the significant difference in body condition I detected between the two ecotypes (Table 8). I found increased eye patch ratio (EPR, a proxy for body condition) values for every age/sex class of BKWs when compared to SRKWs, with particular significance when comparing calves and juveniles (Table 8). While there was no significant difference in the mean EPR of adult females between the two populations, variability in adult female EPR was high (particularly in BKWs), likely as a function of changing reproductive state and the associated burden/release of pregnancy and lactation (Fearnbach et al. 2018).

In the absence of major differences in growth trends or patterns of life history (Olesiuk et al. 2005; Ford et al. 2007; Fearnbach et al. 2011; Towers et al. 2019), I propose that the increased size and body condition of BKWs in comparison to SRKWs is likely a function of

differential prey availability. SRKWs are specialized hunters of salmon with a demonstrated preference for larger Chinook salmon (Ford and Ellis, 2006; Hanson et al. 2010). Declines in the availability of Chinook have been linked to decreased survival (Ford et al. 2009), reproduction (Ward et al. 2009), body size (Fearnbach et al. 2011), and body condition (Fearnbach et al. 2018, 2019; Stewart et al. 2020) in SRKWs, and the population is currently hypothesized to be at least periodically food-limited. Conversely, populations of marine mammal prey items favored by BKWs have seen dramatic increases in abundance in the wake of U.S. and Canadian protections installed in the 1970s. Harbor seal and sea lion abundances have both increased significantly throughout the range of the West Coast Transient BKWs (Trites et al. 2007; Magera et al. 2013; Laake et al. 2018; Ashley et al. 2020), and migrating gray whales have doubled in abundance over the same period (Durban et al. 2015b). This major disparity in food availability between BKWs and SRKWs could fuel the differences in size and body condition observed between the two populations—notably, the 0.4m increase in adult asymptotic size of BKWs corresponds remarkably well with 0.4m declines in the adult sizes of Northern and Southern Resident killer whales (Fearnbach et al. 2011; Groskreutz et al. 2019), which in turn correlate with declining Chinook salmon availability over the same period. It is therefore likely that the disparities in adult sizes of BKWs and Resident killer whales could represent recent responses to environmental conditions. I suggest that the discrepancies in length observed between BKWs and SRKWs are a function of environmental forcing via prey availability, and that the inferred differences in nutritional health underpin their contrasting population dynamics.

This work is coauthored with John Durban, Holly Fearnbach, Lance Barrett-Lennard, and Chloe Kotik. The thesis author was the primary author of this work and led all image and data analysis.

REFERENCES

- Ashley, E.A., Olson, J.K., Adler, T.E., Raverty, S., Anderson, E.M., Jeffries, S., and Gaydos, J.K. (2020) Causes of Mortality in a Harbor Seal (*Phoca vitulina*) Population at Equilibrium. *Front. Mar. Sci.* 7:319. doi: 10.3389/fmars.2020.00319
- Baird, R. and Dill, L., 1995. Occurrence and behaviour of transient killer whales: seasonal and pod-specific variability, foraging behaviour, and prey handling. *Canadian Journal of Zoology*, 73(7), pp.1300-1311.
- Baird, R. and Whitehead, H., 2000. Social organization of mammal-eating killer whales: group stability and dispersal patterns. *Canadian Journal of Zoology*, 78(12), pp.2096-2105.
- Barrett-Lennard, L.G. and Ellis, G.M. 2001. Population structure and genetic variability in Northeastern Pacific killer whales: Towards an assessment of population viability. DFO Can. Sci. Advis. Sec. Res. doc. 2001/065.
- Barrett-Lennard, L.G., Ford, J.K.B, and Heise, K.A. 1996. The mixed blessings of echolocation: differences in sonar use by fish-eating and mammal-eating killer whales. *Anim. Behav.* 51:553-565.
- Bigg, M.A. and Wolman, A.A. 1975. Live-capture killer whale (*Orcinus orca*) fishery, British Columbia and Washington, 1962–1973. *J Fish Res Board Can* 32:1213–1221
- Bigg, M.A., Olesiuk, P.F., Ellis, G.M., Ford, J.K.B., and Balcomb, K.C. III. 1990. Social organization and genealogy of resident killer whales (*Orcinus orca*) in the coastal waters of British Columbia and Washington State. *Rep Int Whal Comm Spec Issue* 12:383–405
- Bigg, M.A. An assessment of killer whale (*Orcinus orca*) stocks off Vancouver Island, British Columbia. Report of the International Whaling Commission. 32:655–66.
- Bradford, A., Weller, D., Punt, A., Ivashchenko, Y., Burdin, A., Van Blaricom, G. and Brownell, R., 2012. Leaner leviathans: body condition variation in a critically endangered whale population. *Journal of Mammalogy*, 93(1), pp.251-266.
- Center for Whale Research, 2016. *Bigg's Killer Whales Transient 2016 ID Guide*. Center for Whale Research.
- Christiansen, F., Dawson, S., Durban, J., Fearnbach, H., Miller, C., Bejder, L., Uhart, M., Sironi, M., Corkeron, P., Rayment, W., Leunissen, E., Haria, E., Ward, R., Warick, H., Kerr, I., Lynn, M., Pettis, H. and Moore, M., 2020. Population comparison of right whale body condition reveals poor state of the North Atlantic right whale. *Marine Ecology Progress Series*, 640, pp.1-16.
- Dawson, S.M., Bowman, M.H., Leunissen, E., and Sirguey, P. 2017. Inexpensive aerial photogrammetry for studies of whales and large marine animals. *Front Mar Sci* 4:366

- Department of Fisheries and Oceans (DFO) Canada. 2007. Recovery Strategy for the Transient Killer Whale (*Orcinus orca*) in Canada [Consultation Draft]. Species at Risk Act Recovery Strategy Series. Fisheries and Oceans Canada, Vancouver 42pp.
- Durban, J.W., Fearnbach, H., Barrett-Lennard, L.G., Perryman, W.L., and Leroi, D.J. 2016. Photogrammetry of killer whales using a small hexacopter launched at sea. *J Unmanned Veh Syst* 3:131–135
- Durban, J., Fearnbach, H., Barrett-Lennard, L., Perryman, W. and Leroi, D., 2015a. Photogrammetry of killer whales using a small hexacopter launched at sea. *Journal of Unmanned Vehicle Systems*, 3(3), pp.131-135.
- Durban, J.W., Weller, D.W., Lang, A.R. and Perryman, W.L., 2015b. Estimating gray whale abundance from shore-based counts using a multilevel Bayesian model. *J. Cetacean Res. Manag.*, 15, pp.61-68.
- Fearnbach, H., Durban, J.W., Ellifrit, D.K., and Balcomb, K.C. III. 2011. Size and long-term growth trends of Endangered fish-eating killer whales. *Endang Species Res* 13: 173–180
- Fearnbach, H., Durban, J.W., Ellifrit, D.K., and Balcomb, K.C. 2018. Using aerial photogrammetry to detect changes in body condition of endangered southern resident killer whales. *Endang Species Res* 35:175–180
- Fearnbach, H., Durban, J.W., Ellifrit, D.K. and Balcomb, K.C., 2018. Using aerial photogrammetry to detect changes in body condition of endangered southern resident killer whales. *Endangered Species Research*, 35, pp.175-180.
- Fearnbach, H., Durban, J.W., Barrett-Lennard, L.G., Ellifrit, D.K. and Balcomb III, K.C., 2019. Evaluating the power of photogrammetry for monitoring killer whale body condition. *Marine Mammal Science*, 36(1), pp.359-364.
- Fiori, L., Doshi, A., Martinez, E., Orams, M. and Bollard-Breen, B., 2017. The Use of Unmanned Aerial Systems in Marine Mammal Research. *Remote Sensing*, 9(6), p.543.
- Ford, J.K.B., and Ellis, G.M. 1999. Transients: mammal-hunting killer whales of British Columbia, Washington and southeastern Alaska. UBC Press, Vancouver.
- Ford, J.K.B., Ellis, G.M. and Balcomb, K.C., 1996. *Killer whales: the natural history and genealogy of Orcinus orca in British Columbia and Washington*. UBC press.
- Ford, J. K.B., Ellis, G. M., Barrett-Lennard, L. G., Morton, A. B., Palm, R. S., & Iii, K. C. B. 1998. Dietary specialization in two sympatric populations of killer whales (*Orcinus orca*) in coastal British Columbia and adjacent waters. *Canadian Journal of Zoology*, 76(8), 1456–1471. doi: 10.1139/cjz-76-8-1456
- Ford, J.K.B., and Ellis, G.M. 2006. Selective foraging by fish-eating killer whales *Orcinus orca* in 638 British Columbia. *Mar Ecol Prog Ser* 316:185–199.
- Ford, J.K.B., Ellis, G.M. and Durban, J.W. 2007. An assessment of the potential for recovery of

West Coast Transient Killer Whales using coastal waters of British Columbia. DFO Can. Sci. Advis. Sec. Res. Doc. 2007/088.

- Ford, J.K.B., Ellis, G.M., Olesiuk, P.F., and Balcomb, K.C. III. 2009. Linking killer whale survival and prey abundance: food limitation in the oceans' apex predator. *Biol Lett* 6:139–142
- Ford, J.K.B, Wright, B., Ellis, G.M., and Candy, J.R. 2009. Chinook salmon predation by resident killer whales: seasonal and regional selectivity, stock identity of prey, and consumption rates. 101. 1-43.
- Groszkreutz, M., Durban, J., Fearnbach, H., Barrett-Lennard, L., Towers, J., & Ford, J. 2019. Decadal changes in adult size of salmon-eating killer whales in the eastern North Pacific. *Endangered Species Research*, 40, 183–188. doi: 10.3354/esr00993
- Hanson, M.B., Baird, R.W., Ford, J.K.B, Hempelmann-Halos, J., Van Doornik, D.M, Candy., J.R., Emmons, C.K, Schorr, G.S, Gisborne, B., Ayres, K.S, Wasser, S.K., Balcomb, K.C., Balcomb-Bortok., K., Sneva, J.G., and Ford., M.J. 2010. Species and stock identification of prey consumer by endangered southern resident killer whales in their summer range. *Endang. Species Res.* 11:69-82.
- Laake, J. L., Lowry, M. S., DeLong, R. L., Melin, S. R., & Carretta, J. V. 2018. Population growth and status of california sea lions. *The Journal of Wildlife Management*, 82(3), 583–595. doi: 10.1002/jwmg.21405
- Laslett, G. M., Eveson, J. P., & Polacheck, T. 2004. Fitting growth models to length frequency data. *ICES Journal of Marine Science*, 61(2), 218–230. doi: 10.1016/j.icesjms.2003.12.006
- Magera, A. M., Flemming, J. E. M., Kaschner, K., Christensen, L. B., & Lotze, H. K. 2013. Recovery Trends in Marine Mammal Populations. *PLoS ONE*, 8(10). doi: 10.1371/journal.pone.0077908
- Miller, C., Best, P., Perryman, W., Baumgartner, M., & Moore, M. 2012. Body shape changes associated with reproductive status, nutritive condition and growth in right whales *Eubalaena glacialis* and *E. australis*. *Marine Ecology Progress Series*, 459, 135–156. doi: 10.3354/meps09675
- Moura, A., Kenny, J., Chaudhuri, R., Hughes, M., Reisinger, R., de Bruyn, P., Dahlheim, M., Hall, N. and Hoelzel, A. 2014. Phylogenomics of the killer whale indicates ecotype divergence in sympatry. *Heredity*, 114(1), pp.48-55.
- Noren, Dawn P. (2011). Estimated field metabolic rates and prey requirements of resident killer whales. Publications, Agencies and Staff of the U.S. Department of Commerce. 296.
- Olesiuk, P.F., Ellis, G.M., and Ford, J.K.B. 2005. Life history and population dynamics of

- northern resident killer whales (*Orcinus orca*) in British Columbia. Res Doc 2005/45. Canadian Science Advisory Secretariat, Fisheries and Oceans Canada, Ottawa.
- Parsons, K.M., Durban, J.W., Burdin, A.M., Burkanov, V.N., Pitman, R.L., Barlow, J., Barrett-Lennard, L.G., LeDuc, R.G., Robertson, K.M., Matkin, C.O. and Wade, P.R., 2013. Geographic patterns of genetic differentiation among killer whales in the northern North Pacific. *Journal of Heredity*, 104(6), pp.737-754.
- Pettis, H. M., Rolland, R. M., Hamilton, P. K., Brault, S., Knowlton, A. R., & Kraus, S. D. 2004. Visual health assessment of North Atlantic right whales (*Eubalaena glacialis*) using photographs. *Canadian Journal of Zoology*, 82(1), 8–19. doi: 10.1139/z03-207
- Perryman, W.L. and Lynn, M.S., 2002. Evaluation of nutritive condition and reproductive status of migrating gray whales (*Eschrichtius robustus*) based on analysis of photogrammetric data. *Journal of Cetacean Research and Management*, 4(2), pp.155-164.
- Pitman, R.L., Perryman, W.L., LeRoi, D. and Eilers, E., 2007. A dwarf form of killer whale in Antarctica. *Journal of Mammalogy*, 88(1), pp.43-48.
- Richards, F.J. 1959. A flexible growth function for empirical use. *Journal of Experimental Botany* **10**, 290-300.
- Robeck, T., & Monfort, S. 2006. Characterization of male killer whale (*Orcinus orca*) sexual maturation and reproductive seasonality. *Theriogenology*, 66(2), 242–250. doi: 10.1016/j.theriogenology.2005.11.007
- Ross P.S., Ellis GM, Ikonomou MG, Barrett-Lennard LG, Addison RF. 2000. High PCB concentrations in free-ranging pacific killer whales, *Orcinus orca*: effects of age, sex and dietary preference. *Marine Pollution Bulletin* 40(6): 504-515.
- Ross, P. S. 2006. Fireproof killer whales (*Orcinus orca*): flame-retardant chemicals and the conservation imperative in the charismatic icon of British Columbia, Canada. *Canadian Journal of Fisheries and Aquatic Sciences*, 63(1), 224–234. doi: 10.1139/f05-244
- Saulitis, E., Matkin, C., Barrett-Lennard, L., Heise, K., and Ellis., G. 2000. Foraging strategies of sympatric killer whale (*Orcinus orca*) populations in Prince William Sound, Alaska. *Mar. Mamm. Sci.* 16(1):94-109.
- Towers, J.R., Sutton, G.J., Shaw, T.J.H., Malleson, M., Matkin, D., Gisborne, B., Forde, J., Ellifrit, D., Ellis, G.M., Ford, J.K.B., and Doniol-Valcroze, D. 2019. Photo-identification Catalogue, Population Status, and Distribution of Bigg’s Killer Whales known from Coastal Waters of British Columbia, Canada. *Can. Tech. Rep. Fish. Aquat. Sci.* 3311: vi + 299p.
- Trites, A.W., Deecke, V.B., Gregr, E.J., Ford, J.K. and Olesiuk, P.F., 2007. Killer whales,

whaling, and sequential megafaunal collapse in the North Pacific: a comparative analysis of the dynamics of marine mammals in Alaska and British Columbia following commercial whaling. *Marine mammal science*, 23(4), pp.751-765.

Stewart, J.D., Durban, J.W., Fearnbach, H., Barrett-Lennard, L.G., Casler, P.K., Ward, E.J and Dapp, D.R. 2020. Survival of the Fattest: Using aerial photogrammetry to monitor nutritional stress in killer whales. In review, *Science Advances*.

Ward, E.J., Holmes, E.E., and Balcomb, K.C. 2009. Quantifying the effects of prey abundance on killer whale reproduction. *J Appl Ecol* 46:632–640.